

ELECTRONIC SUPPLEMENTARY INFORMATION

Twisted Biaryl-Amines as Novel Host Materials for Green-Emissive Phosphorescent Organic Light-Emitting Diodes (PhOLEDs)

Samik Jhulki,^a Avijit Ghosh,^b Tahsin J. Chow^{b,*} and Jarugu Narasimha Moorthy^{a,*}

^a*Department of Chemistry, Indian Institute of Technology, Kanpur 208016, INDIA*

^b*Institute of Chemistry, Academia Sinica, Taipei, Taiwan 115, Republic of China*

E-Mail: moorthy@iitk.ac.in

Table of Contents

1	General Aspects and details of quantum yield, electrochemical measurements and device fabrications	S3-S5
2	Scheme for the synthesis of biaryl cores	S5
3	PL of vacuum sublimed films of TetMeTPA , TetOMeTPA , TetMeCZL and TetOMeCZL	S6
4	CVs of the hosts	S6
5	TGA profiles of the hosts	S7
6	DSC profiles of the hosts	S7
7	EL spectra at different voltages for the devices of configuration A	S8
8	Plots of external quantum efficiency vs. current density, external quantum efficiency vs. luminance, luminous efficiency vs. current density, luminous efficiency vs. luminance, power efficiency vs. current density and power efficiency vs. luminance for the devices of configuration A	S9
9	EL spectra at different voltages for the devices of configuration B	S10
10	Plots of external quantum efficiency vs. current density, external quantum efficiency vs. luminance, luminous efficiency vs. current density, luminous efficiency vs. luminance, power efficiency vs. current density and power efficiency vs. luminance for the devices of configuration B	S11
11	EL spectra at different voltages for the devices of TetMeTPA for the configuration C	S12
12	Plots of external quantum efficiency vs. current density, external quantum efficiency vs. luminance, luminous efficiency vs. current density, luminous efficiency vs. luminance, power efficiency vs. current density and power	S13

	efficiency vs. luminance for the devices of TetMeTPA with configuration C	
13	¹ H and ¹³ C NMR spectra of 3,3'-diiodo-2,2',6,6'-tetramethoxybiphenyl in CDCl ₃	S14
14	¹ H and ¹³ C NMR spectra of 3,3'-diiodo-2,2',6,6'-tetramethylbiphenyl in CDCl ₃	S15
15	¹ H and ¹³ C NMR spectra of TetMeTPA in CDCl ₃ .	S16
16	¹ H and ¹³ C NMR spectra of TetOMeTPA in CDCl ₃ .	S17
17	¹ H and ¹³ C NMR spectra of TetMeCZL in CDCl ₃ .	S18
18	¹ H and ¹³ C NMR spectra of TetOMeCZL in CDCl ₃ .	S19
19	References	S20

EXPERIMENTAL SECTION

General Aspects. ^1H NMR spectra were recorded on JEOL (400/500 MHz) spectrometers in CDCl_3 as a solvent. ^{13}C NMR spectra were recorded on JEOL-Lambda (100/125 MHz) spectrometers with complete proton decoupling. ESI and EI mass spectra analyses were carried out on Waters $^{\text{Q}}$ TOF and GCT premier mass spectrometers, respectively. IR spectra were recorded on a Bruker Vector 22 FT-IR spectrophotometer. X-ray powder patterns were recorded on a Rigaku X-ray diffractometer. The TGA and DSC measurements were carried out using Mettler-Toledo and SDT Q600 instruments, respectively, at $10\text{ }^\circ\text{C}/\text{min}$ under a nitrogen gas atmosphere. UV-Vis absorption spectra were recorded on a Shimadzu UV-1800 spectrophotometer. PL measurements in solution and solid state were carried out using FluoroMax-4; FM4-3000 spectrofluorimeter, Horiba Scientific. Cyclic voltammetry measurements were performed using CHI610E electrochemical work-station (CH instruments, Texas, USA). All solvents were distilled prior to use, and HPLC grade solvents used for UV-vis and PL measurements were procured from Merck. Column chromatography was conducted with silica-gel of 100-200 μ mesh.

Materials. The starting compounds, namely, 2,2',6,6'-tetramethoxybiphenyl¹ and 2,2',6,6'-tetramethylbiphenyl², and the boronic acids, namely, (4-(diphenylamino)phenyl)boronic acid³ and (4-(9H-carbazol-9-yl)phenyl)boronic acid⁴, were synthesized following literature reported procedures. ITO-coated glass slides of thickness 0.7 mm and resistance 11 Ω , and materials such as HAT-CN, NPB, TAPC, CBP, TmPyPB, Ir(ppy)₃, LiF and Al, which were employed for device fabrications, were procured from commercial sources.

PL Quantum Yield Measurements (Solution State). UV-Vis and photoluminescence spectra of dilute DCM solutions (ca. 1×10^{-5} M) of the compounds were recorded for the determination of fluorescence quantum yields. Quantum yields were calculated by a relative method using anthracene as the standard; quantum yield for the latter in cyclohexane is 0.36 [5]. The quantum yields of the compounds were calculated using the following equation:

$$\Phi_u = \Phi_s(A_s/A_u) (I_u/I_s) (\eta_u/\eta_s)^2$$

where:

Φ_s ~ quantum yield of the standard

A_u ~ absorbance of the unknown sample at the excitation wavelength

A_s ~ absorbance of the standard sample at the excitation wavelength

I_u ~ integrated emission intensities of the sample

I_s ~ integrated emission intensities of the standard

η_u ~ refractive index of the unknown solution (pure solvent is a reasonable approximation)

η_s ~ refractive index of the standard solution (pure solvents is assumed)

Electrochemical Measurements. The cyclic voltammetry experiments were carried out in a typical 3-electrode compartment cell using a Ag/AgCl reference electrode, a Pt wire counter electrode and a Pt working electrode. The cell containing solution of the sample (1 mM) and the supporting electrolyte (0.1 M, tetrabutylammonium hexafluorophosphate) was degassed thoroughly with nitrogen gas before scanning for redox properties. Ferrocene (HOMO = -4.8 eV with respect to vacuum) was used as an internal standard; ferrocene/ferrocenium (Fc/Fc⁺) redox couple displays a half cell potential at 0.45 V. The oxidation potentials of the compounds were subsequently calculated from either half cell or onset oxidation potentials. The HOMO energy in each case was calculated with reference to the ferrocene oxidation potential by using the following general equation:

$$E_{\text{HOMO}} = -[(E_{(\text{ox})} - E_{1/2, \text{Fc}/\text{Fc}^+}) + 4.8] \text{ eV}$$

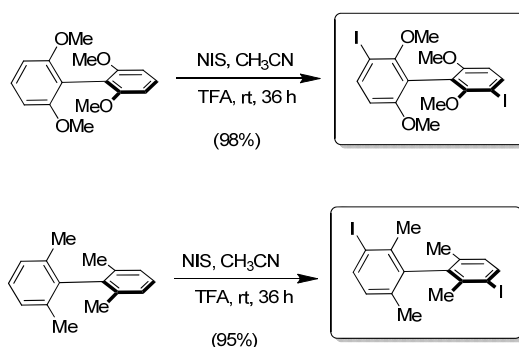
where, $E_{(\text{ox})}$ refers to either half cell potential of the first oxidation peak in the case of reversible oxidation, or onset oxidation potential in the case of irreversible oxidation.

The LUMO energies were obtained by subtraction of the band gap energies from the HOMO energies. The band gap energies for the compounds were in turn calculated from the red edge absorption wavelength.

$$E_{\text{LUMO}} = E_{\text{HOMO}} - E_g^{\text{opt}}$$

Device Fabrications. The patterned ITO-coated glass slides were cleaned rigorously by sonication sequentially in a detergent solution, distilled water (4 times), isopropanol and acetone for 15 min each. Subsequently, they were dried in a flow of nitrogen and further cleaned by three cycles of oxygen plasma treatment (All Real Tech. PCD150) at 45 W for 5 min. The cleaned ITO-coated glasses were transferred to a vacuum chamber (10^{-5} to 10^{-6} torr), and placed in a rotating holder firmly. Organic layers and metals were deposited at a rate of 0.4–1.0 and 8–10 Å/s, respectively. The thickness of each layer was monitored by a quartz thickness controller placed near the rotating disk. After completion of the evaporation without breaking the vacuum, the devices were sealed by cover-glasses containing UV-cured epoxy glue at the periphery. The I-V-L characteristics and other measurements of the devices thus made were performed using a Keithly 2400 source meter connected to a PR650 spectrophotometer.

Scheme S1. Synthesis of the core scaffolds.



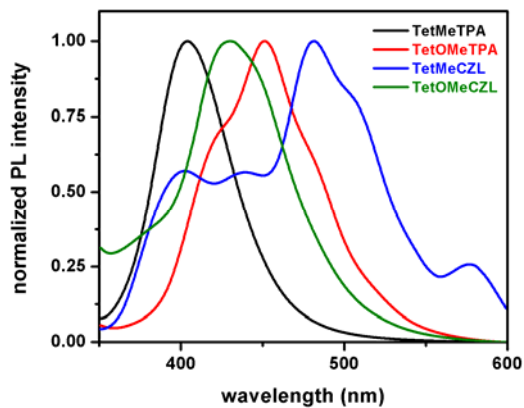


Fig. S1. Normalized PL emission spectra of vacuum sublimed films of **TetMeTPA**, **TetOMeTPA**, **TetMeCZL** and **TetOMeCZL** when excited at 325 nm; for **TetMeCZL**, the excitation wavelength was 275 nm.

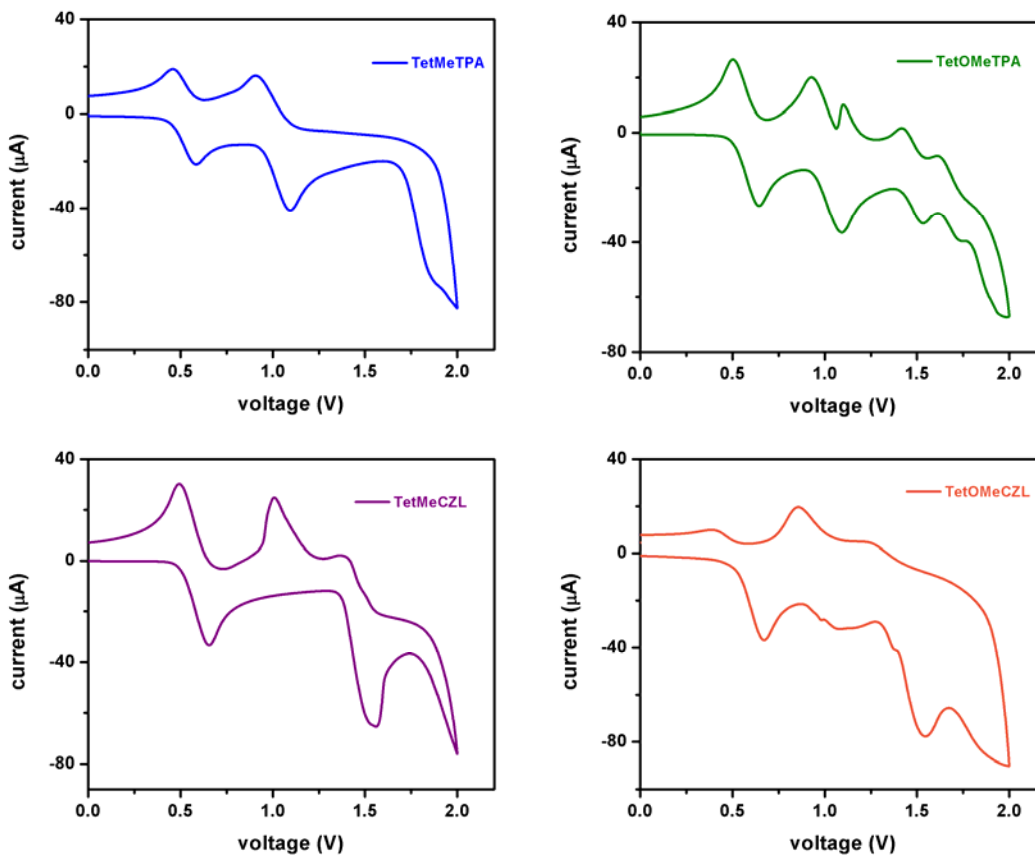


Fig. S2. Cyclic voltammograms of **TetMeTPA**, **TetOMeTPA**, **TetMeCZL** and **TetOMeCZL** in DCM using $n\text{-Bu}_4\text{NPF}_6$ as the supporting electrolyte.

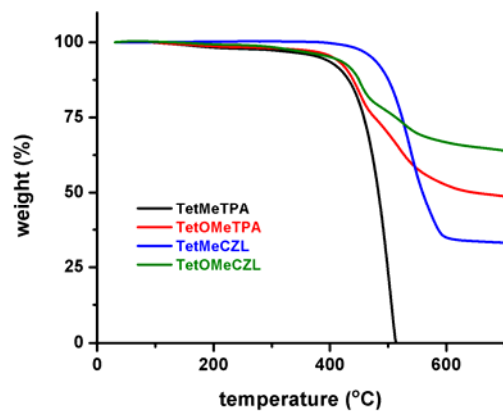


Fig. S3. TGA profiles of the hosts.

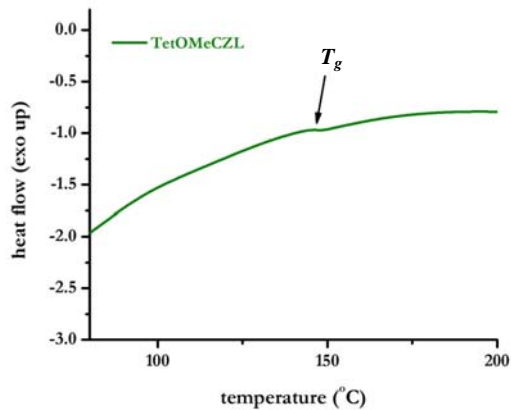
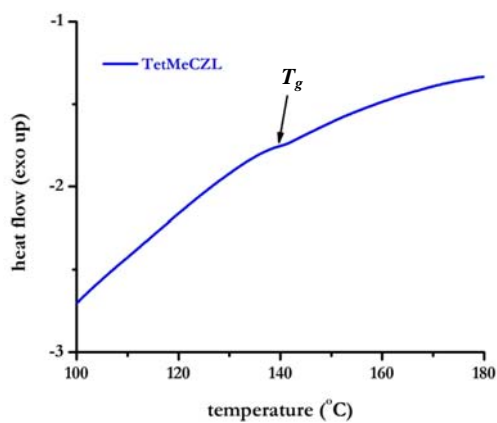
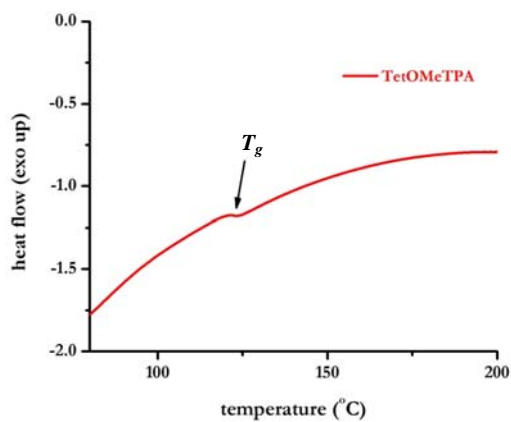
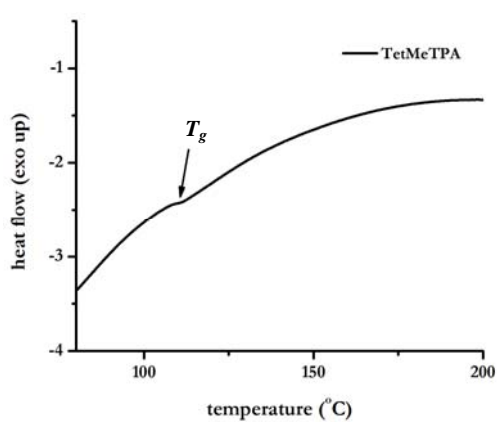


Fig. S4. DSC profiles of the hosts.

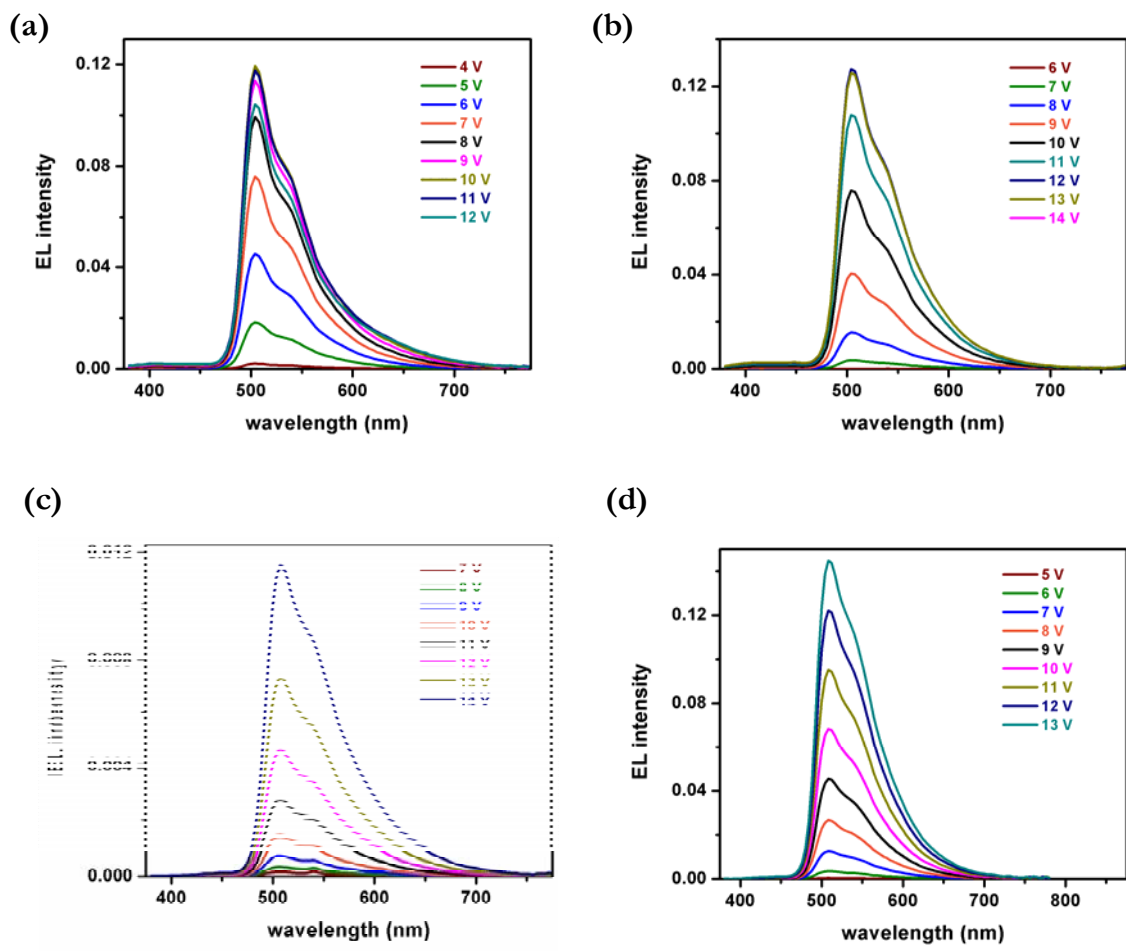


Fig. S5. EL spectra at different voltages for the devices of configuration A with **TetMeTPA**(a), **TetOMeTPA**(b), **TetMeCZL** (c) and **TetOMeCZL**(d) as hosts.

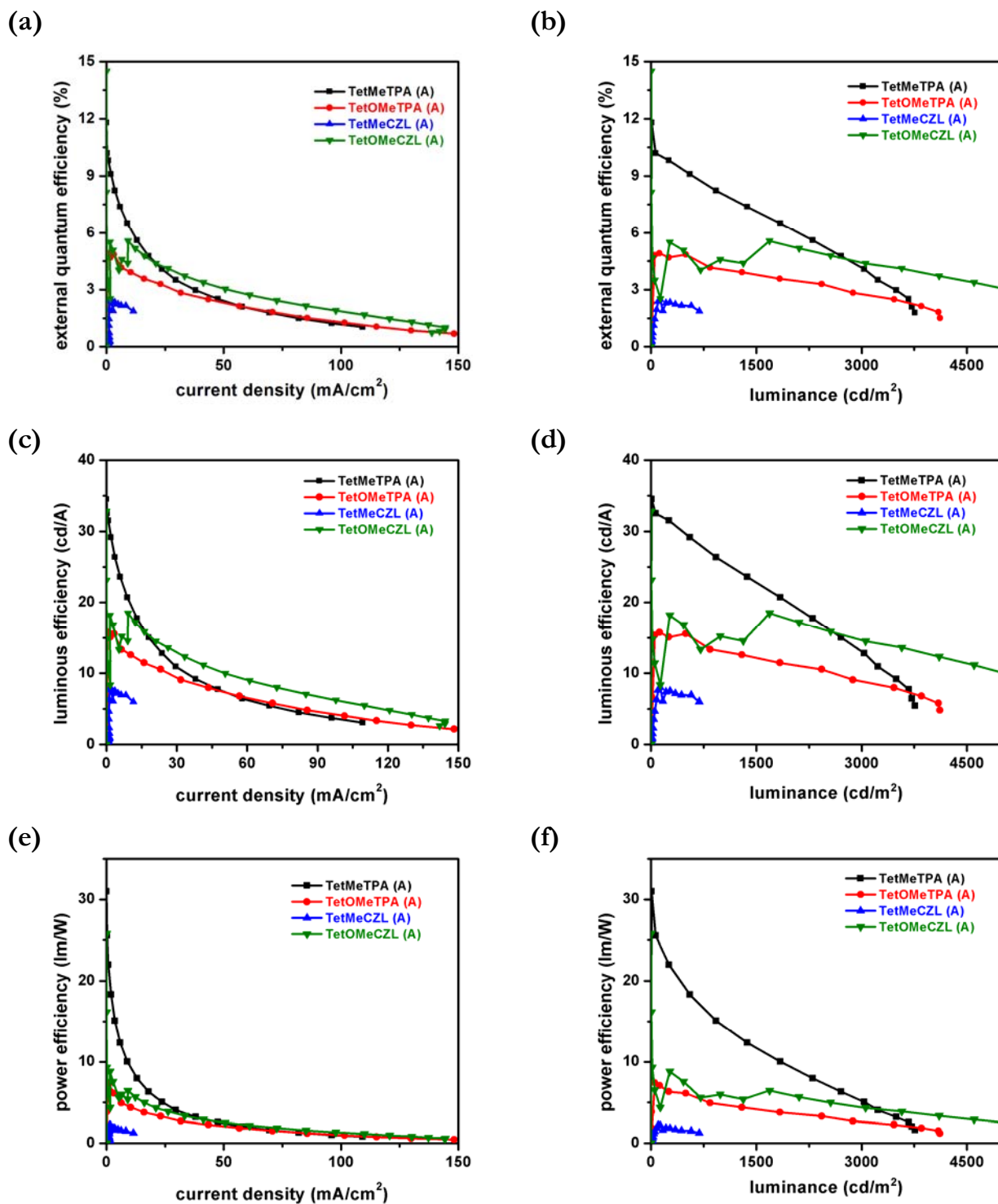


Fig. S6. Plots of external quantum efficiency vs. current density (a), external quantum efficiency vs. luminance (b), luminous efficiency vs. current density (c), luminous efficiency vs. luminance (d), power efficiency vs. current density (e) and power efficiency vs. luminance (f) for the devices of configuration A, refer to text.

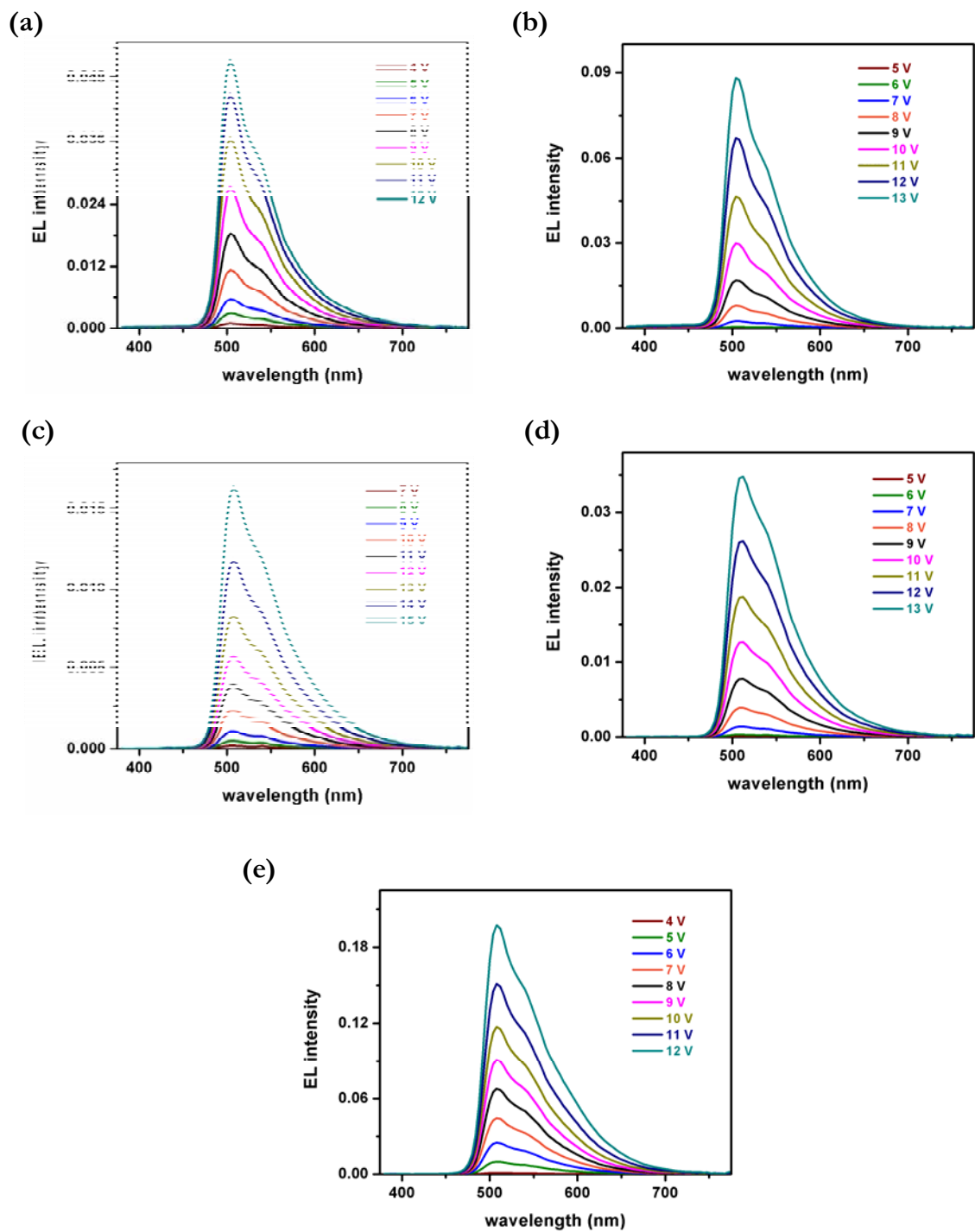


Fig. S7. EL spectra at different voltages for the devices of configuration B with **TetMeTPA** (a), **TetOMeTPA** (b), **TetMeCZL** (c), **TetOMeCZL** (d) and **CBP** (e) as hosts.

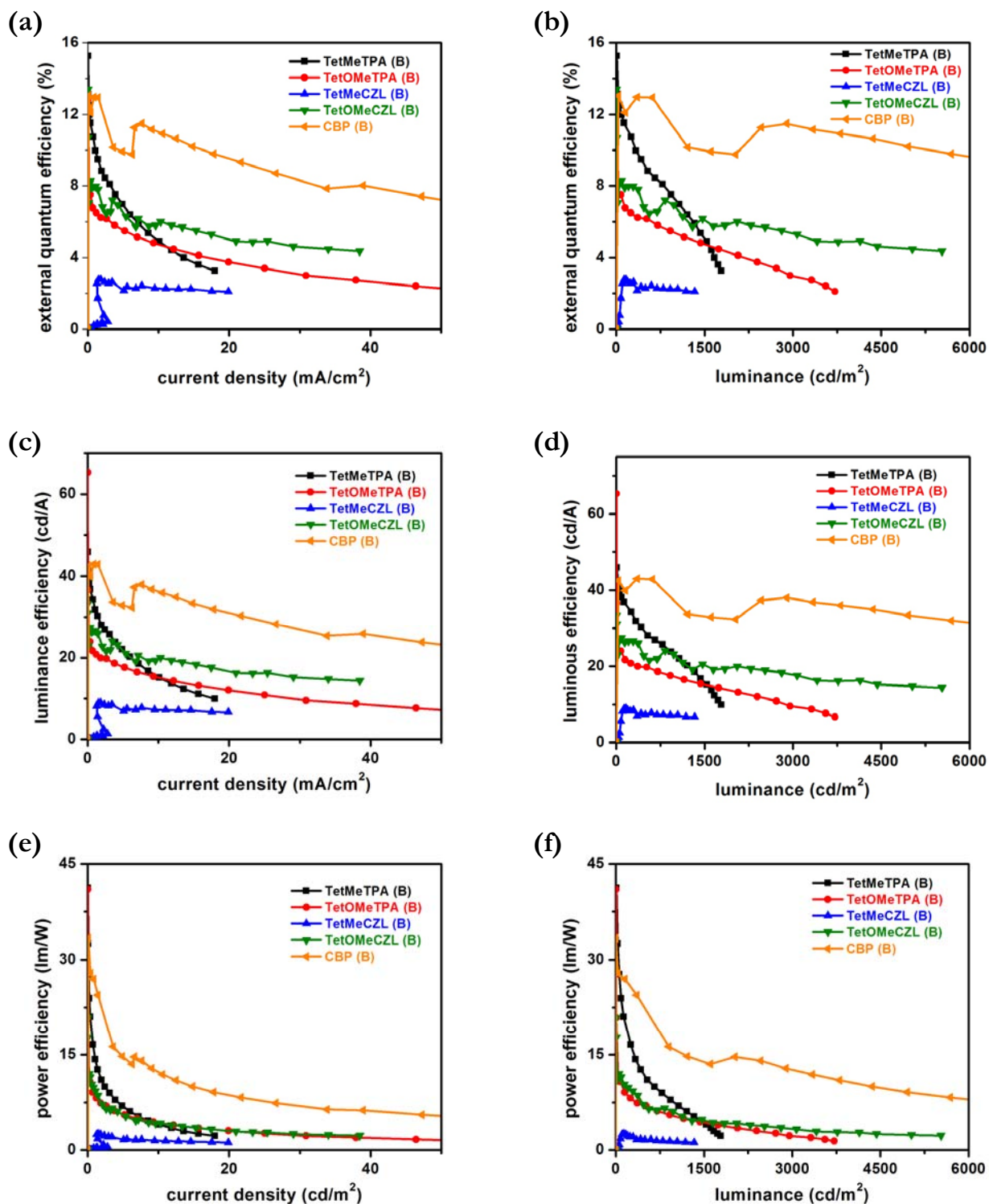


Fig. S8. Plots of external quantum efficiency vs. current density (a), external quantum efficiency vs. luminance (b), luminous efficiency vs. current density (c), luminous efficiency vs. luminance (d), power efficiency vs. current density (e) and power efficiency vs. luminance (f) for the devices of configuration B, refer to text.

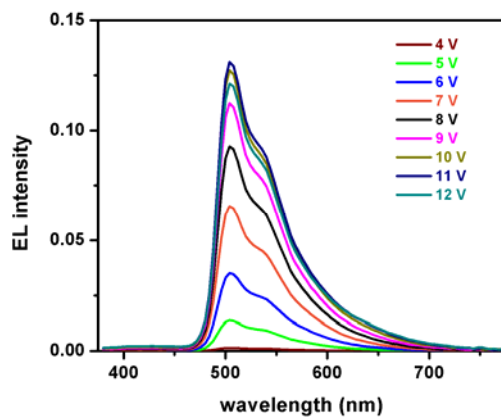


Fig. S9. EL spectra at different voltages for the devices of **TetMeTPA** for the configuration: ITO/TAPC (45 nm)/**TetMeTPA**:Ir(ppy)₃ (7-8%, 30 nm)/TmPyPB (45 nm)/LiF (2 nm)/Al (150 nm).

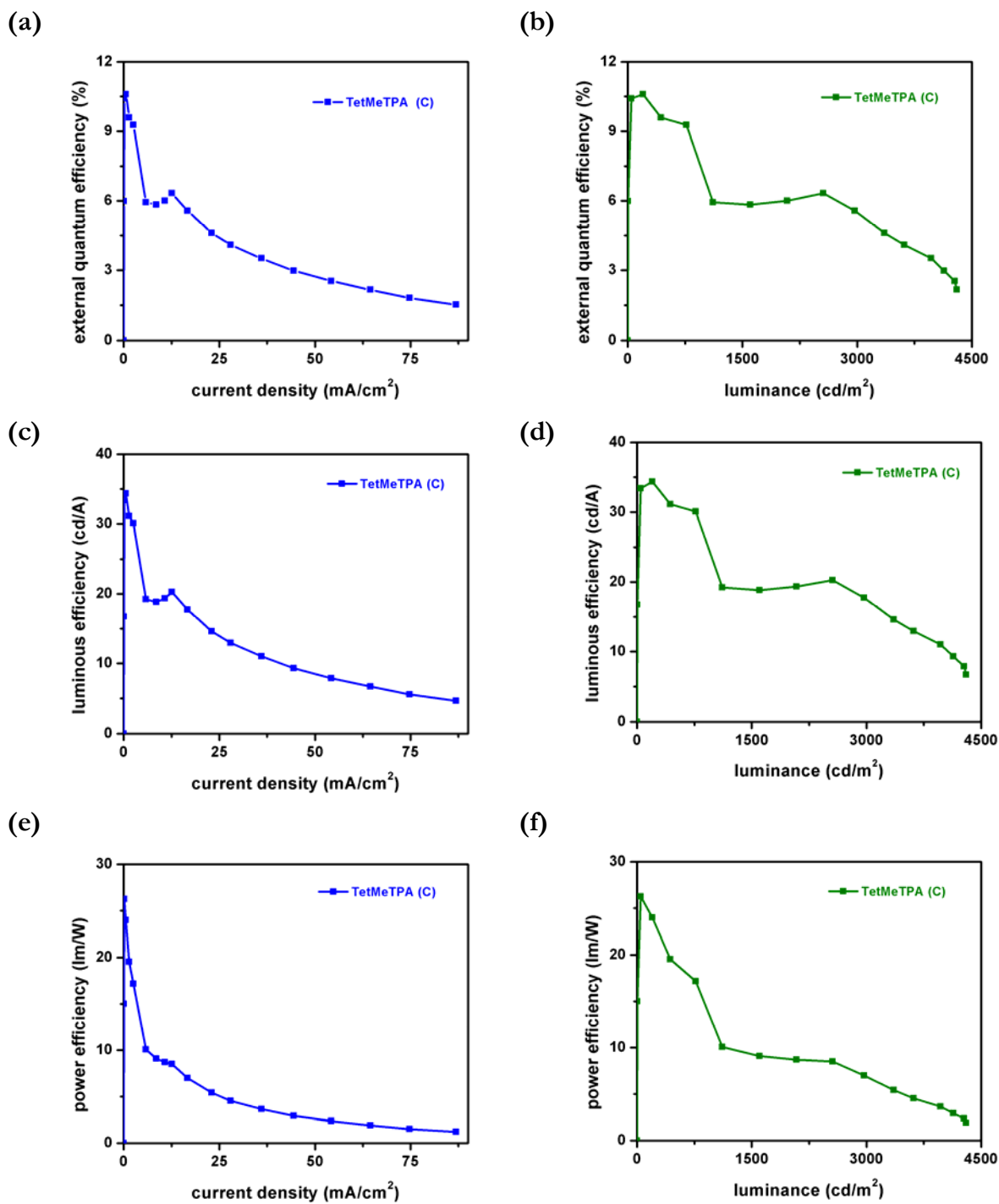


Fig. S10. Plots of external quantum efficiency vs. current density (a), external quantum efficiency vs. luminance (b), luminous efficiency vs. current density (c), luminous efficiency vs. luminance (d), power efficiency vs. current density (e) and power efficiency vs. luminance (f) for the devices of **TetMeTPA** with configuration C, refer to text.

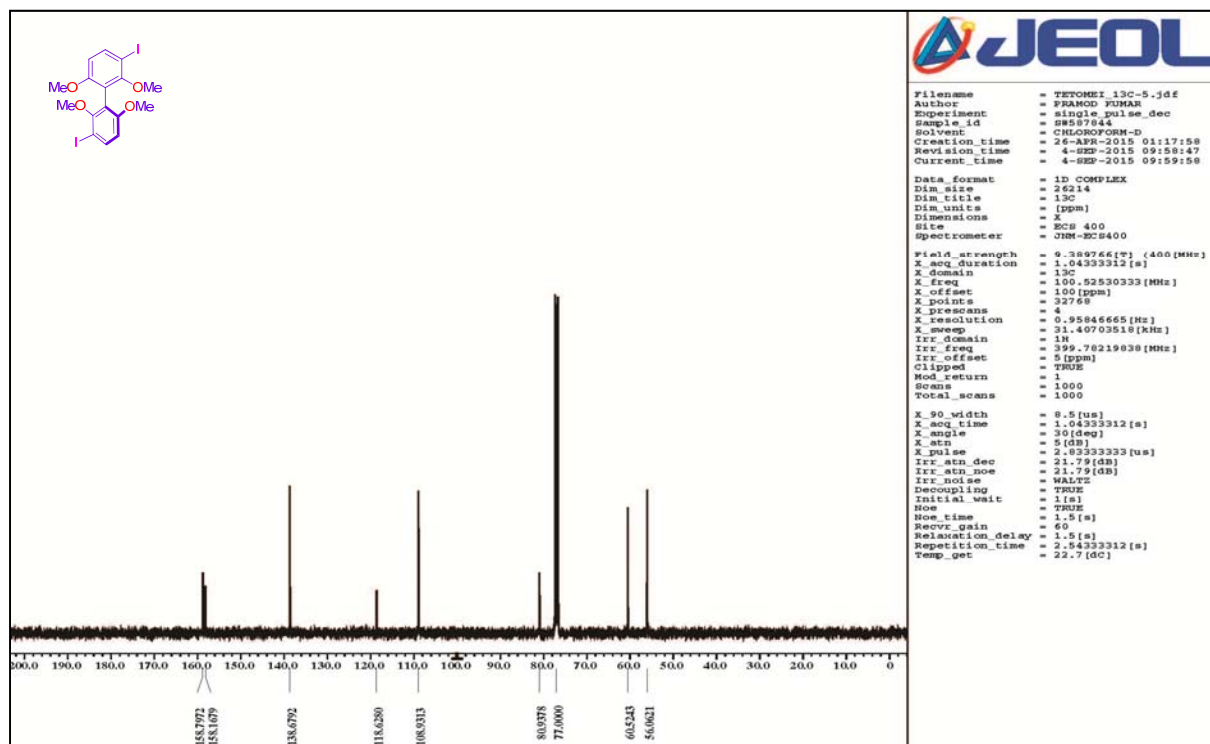
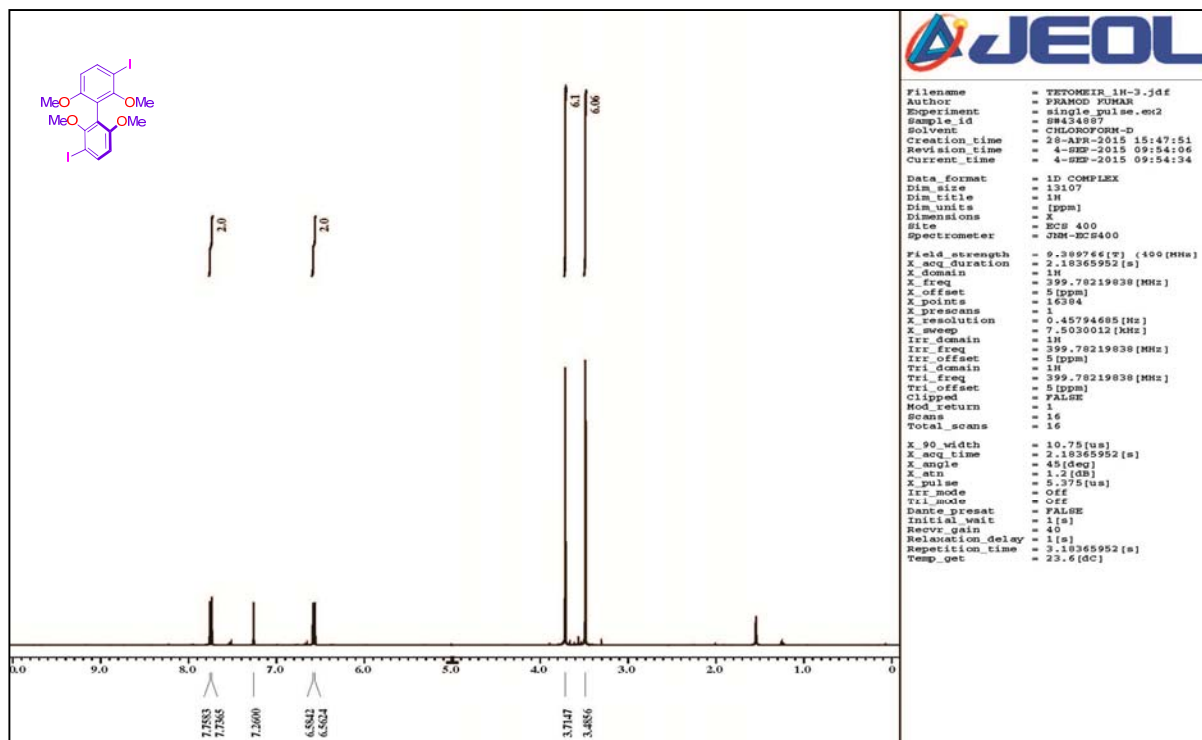


Fig. S11. ^1H (400 MHz) and ^{13}C (100 MHz) NMR spectra of 3,3'-diiodo-2,2',6,6'-tetramethoxybiphenyl in CDCl_3 .

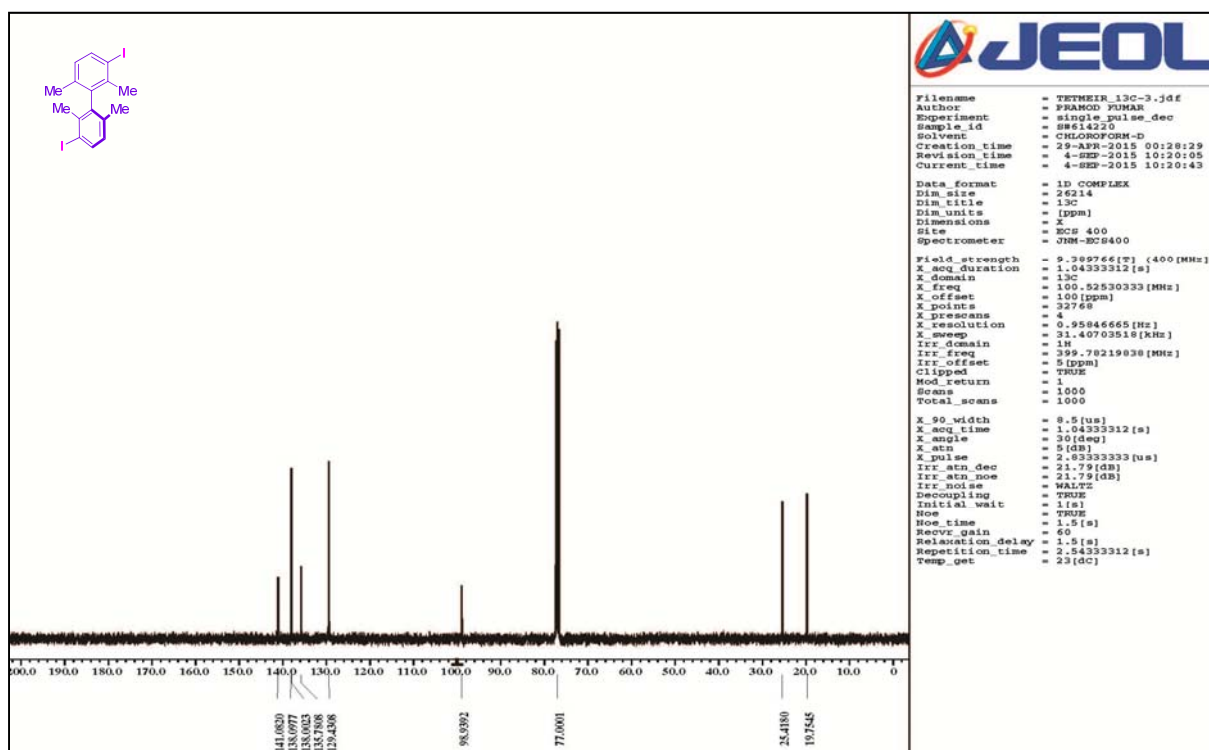
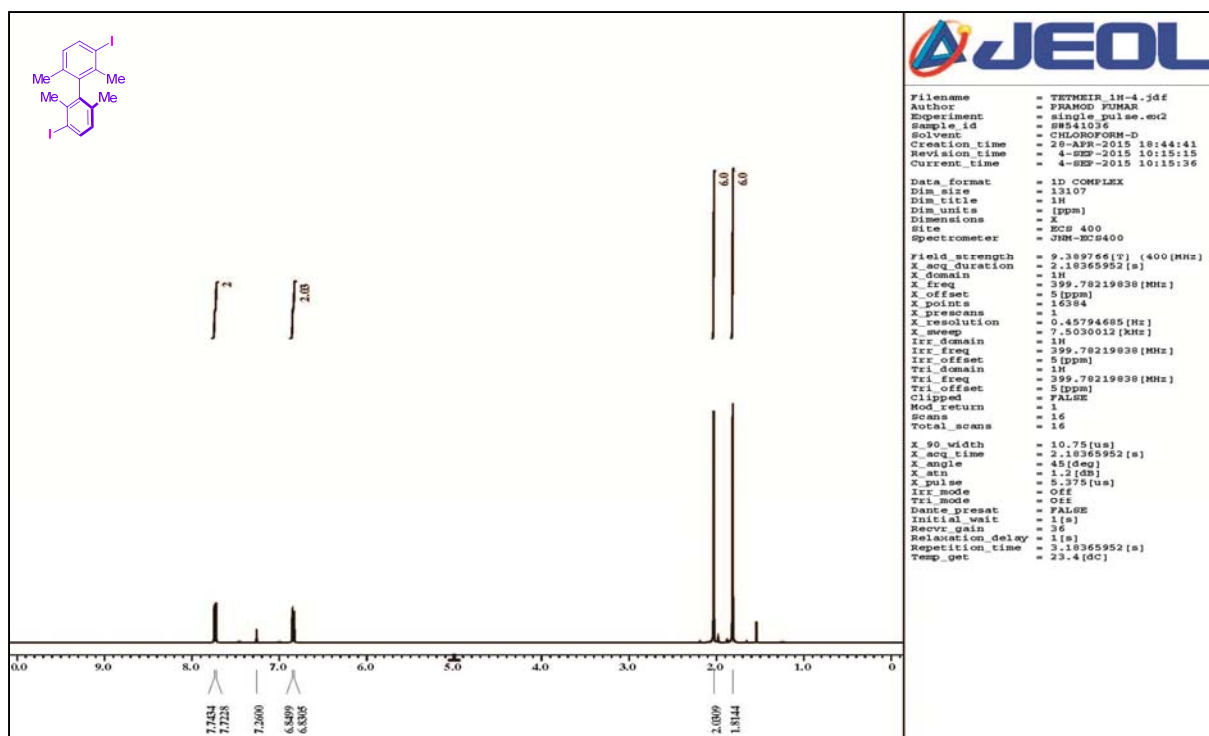


Fig. S12. ¹H (500 MHz) and ¹³C (125 MHz) NMR spectra of 3,3'-diiodo-2,2',6,6'-tetramethylbiphenyl in CDCl₃.

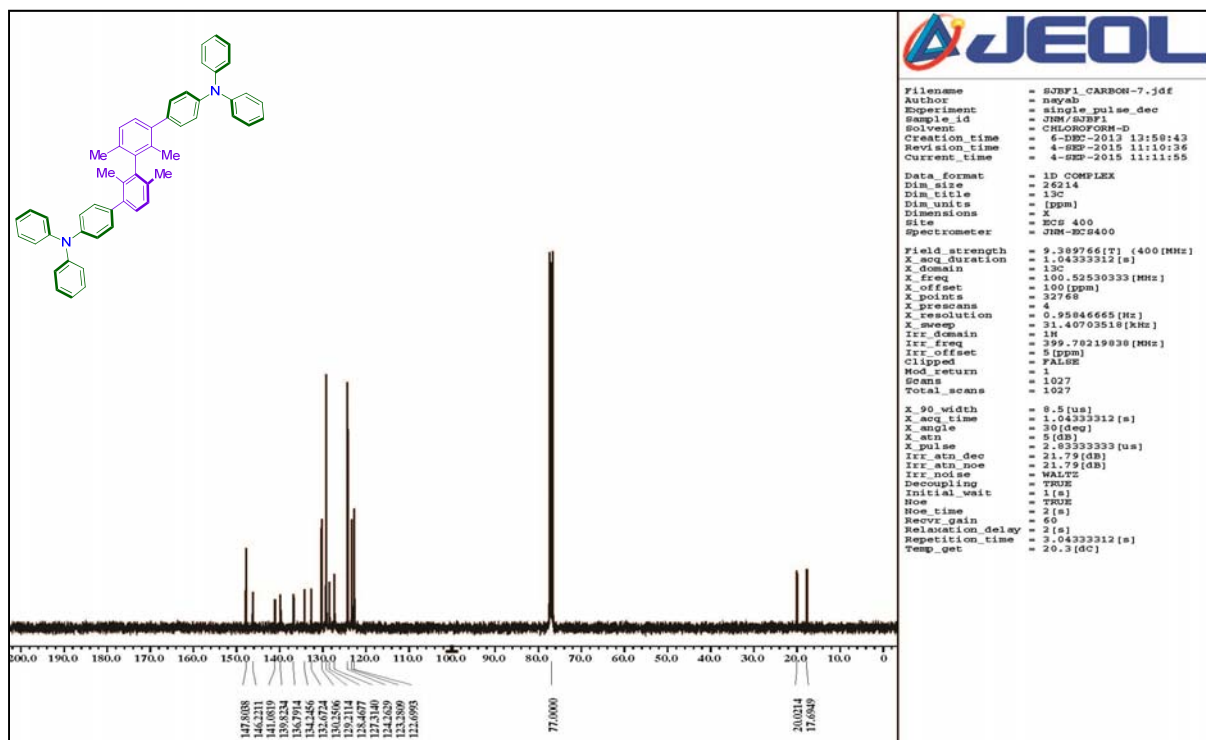
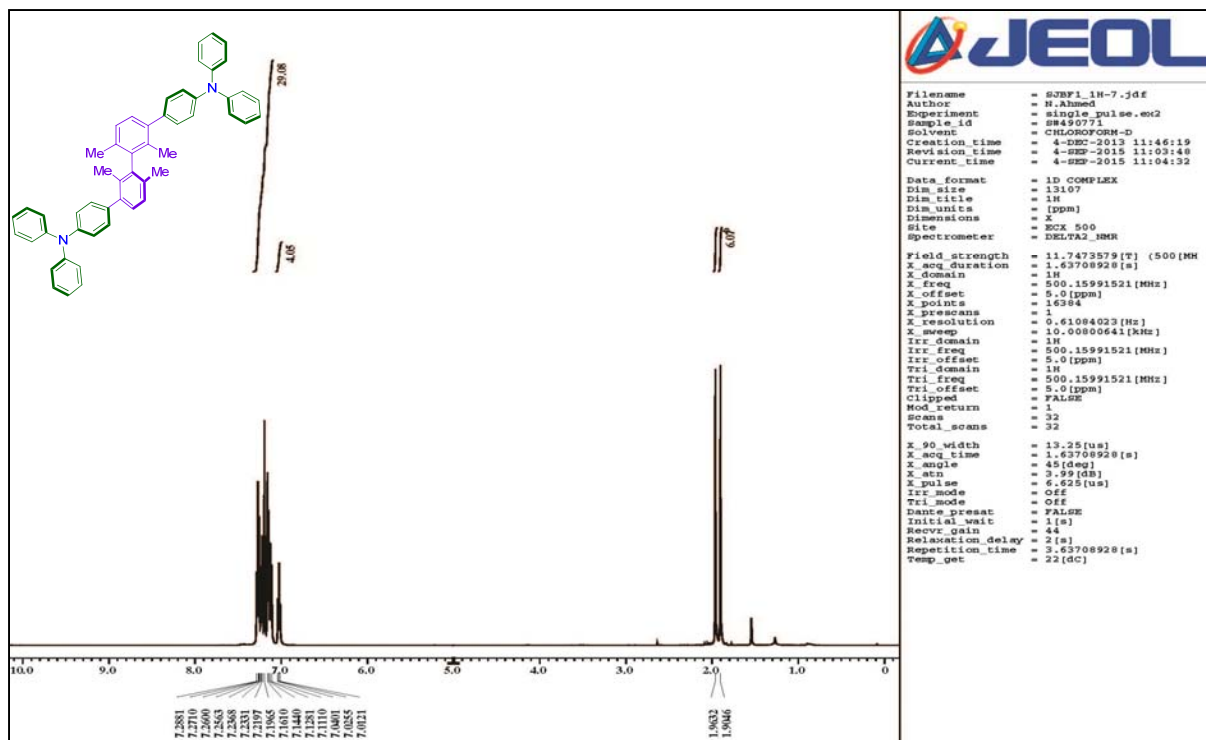


Fig. S13. ^1H (500 MHz) and ^{13}C (100 MHz) NMR spectra of TetMeTPA in CDCl_3 .

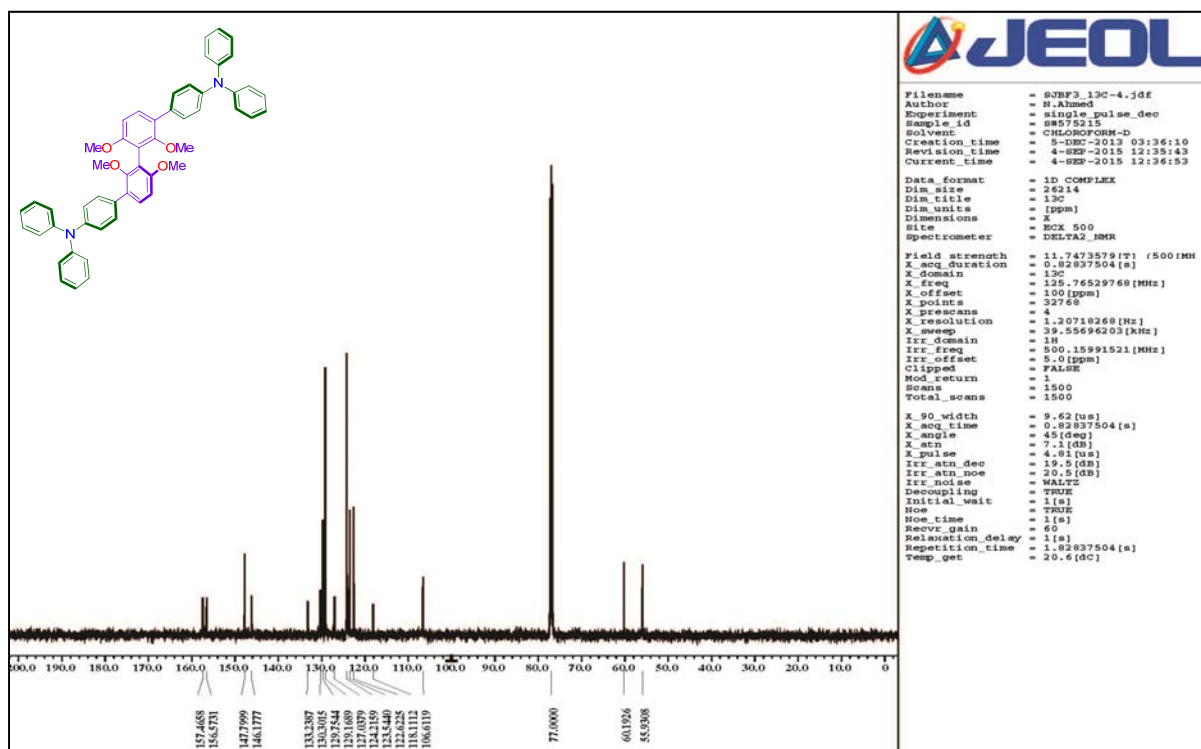
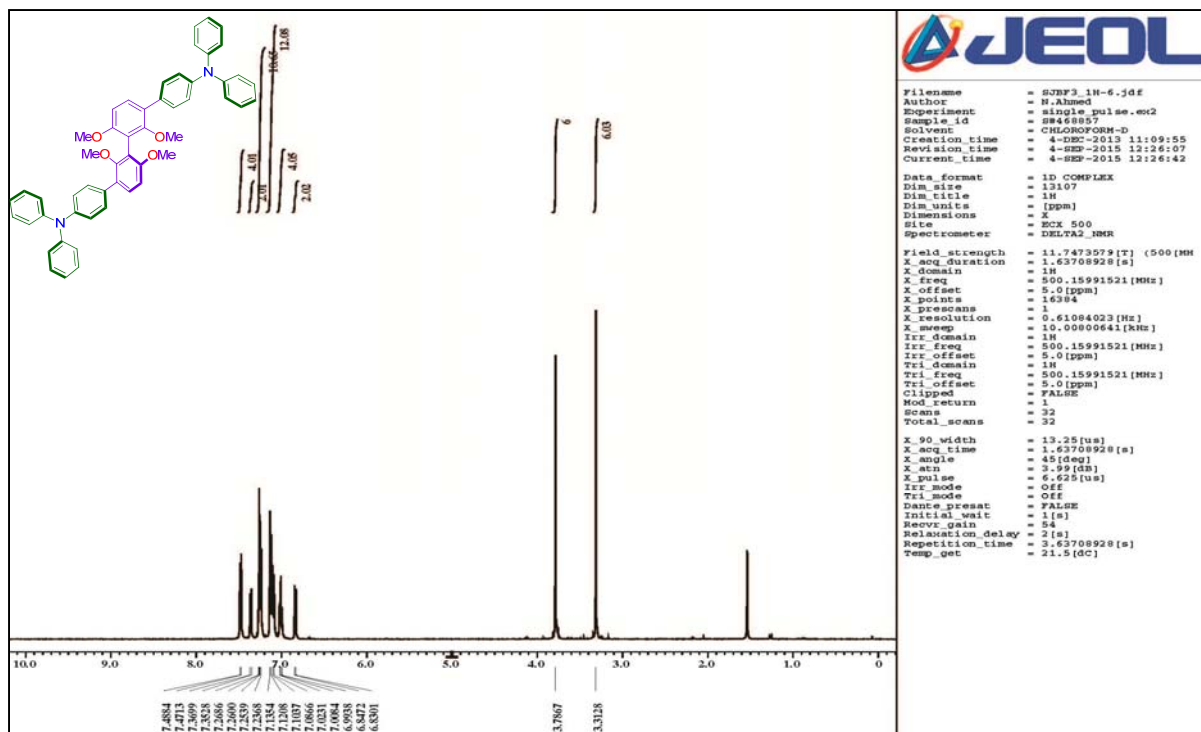


Fig. S14. ^1H (500 MHz) and ^{13}C (125 MHz) NMR spectra of TetOMeTPA in CDCl_3 .

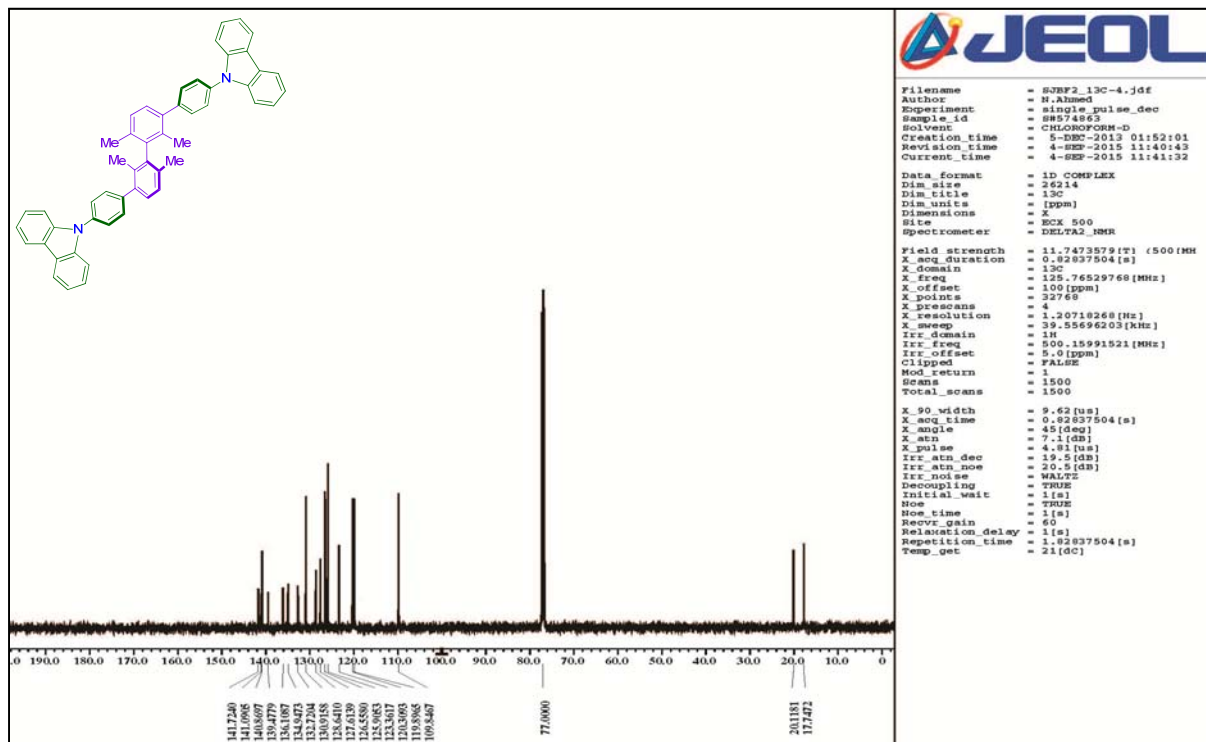
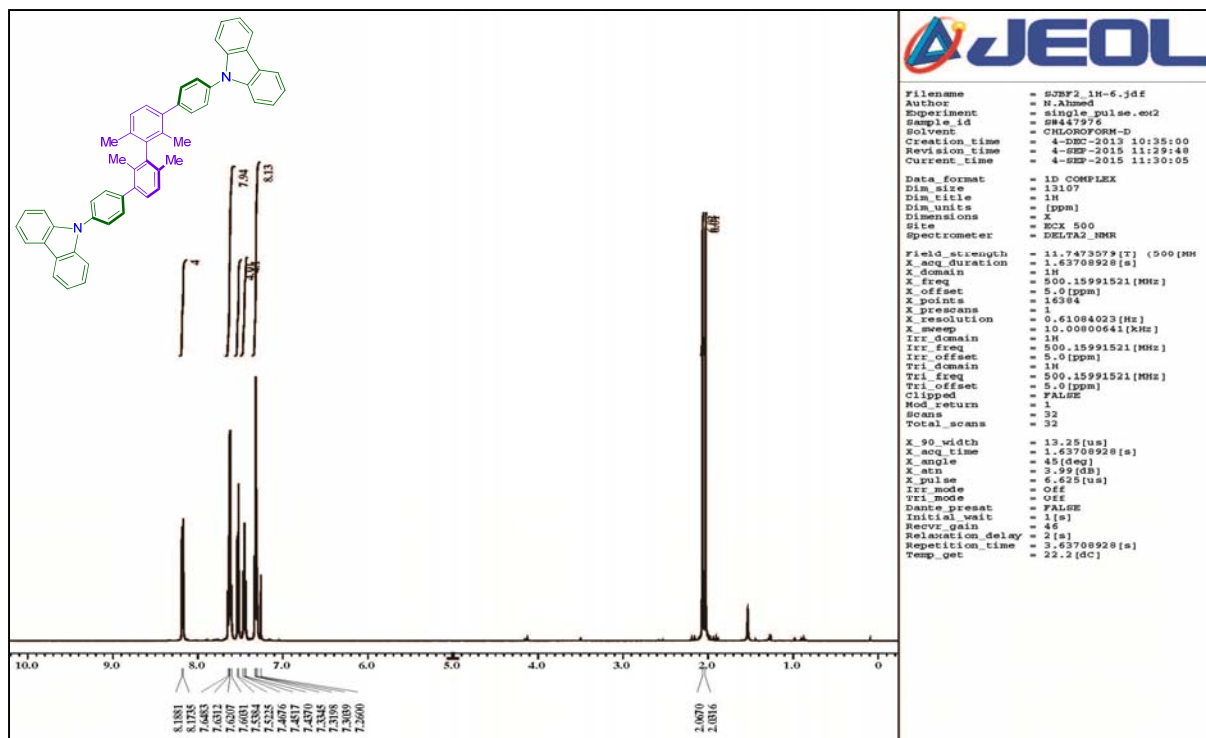


Fig. S15. ^1H (500 MHz) and ^{13}C (125 MHz) NMR spectra of **TetMeCZL** in CDCl_3 .

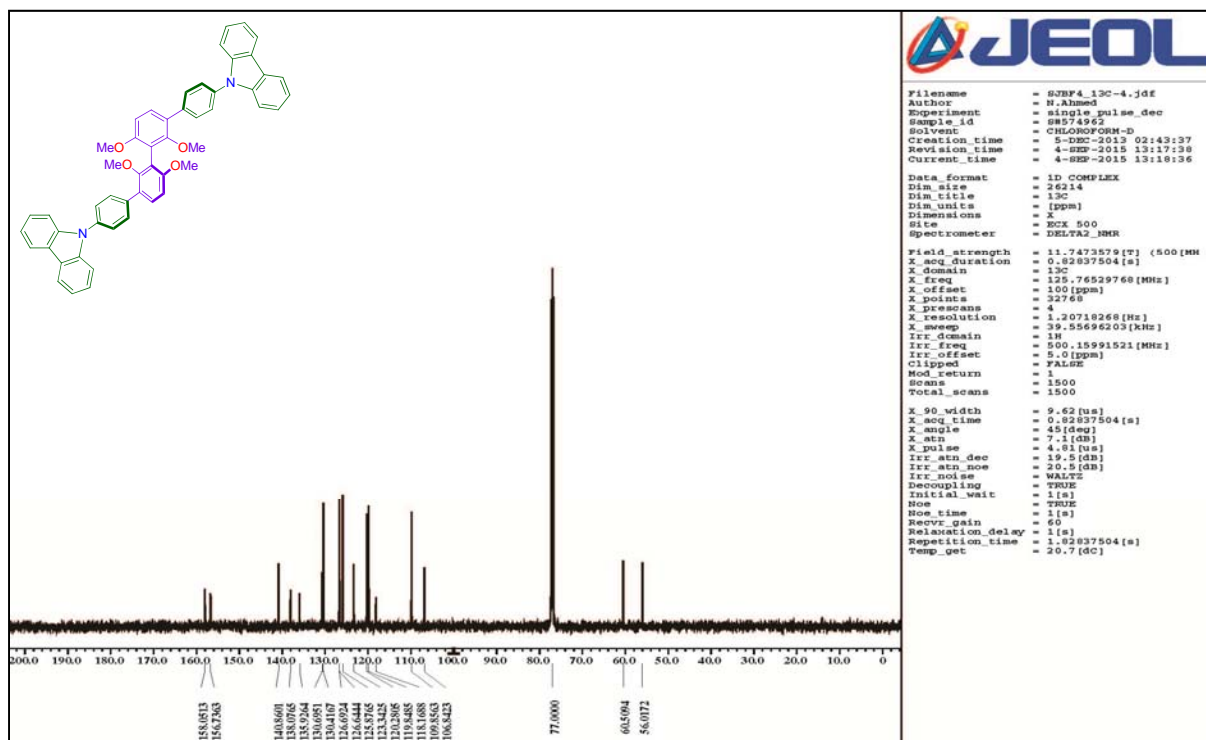
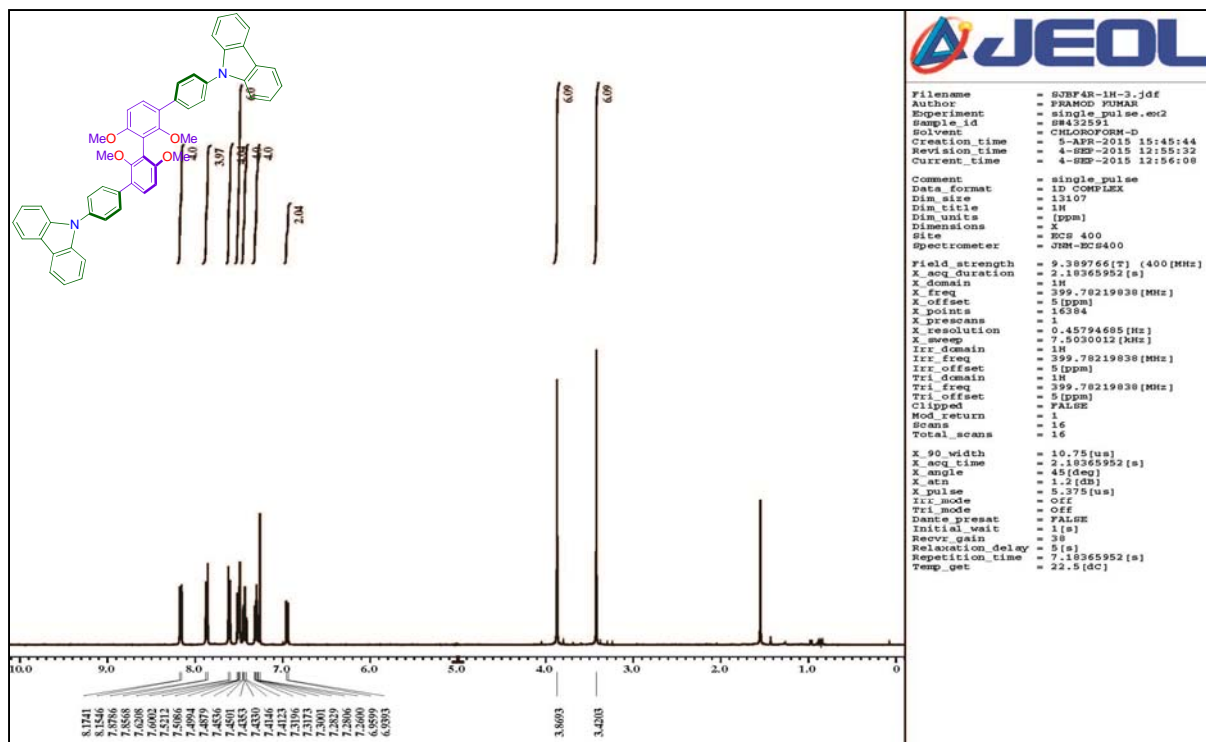


Fig. S16. ¹H (400 MHz) and ¹³C (125 MHz) NMR spectra of TetOMeCZL in CDCl₃.

References

- 1 S. Seth, P. Venugopalan and J. N. Moorthy, *Chem. –Eur. J.*, 2015, **21**, 2241.
- 2 S. Seth, G. Savitha and J. N. Moorthy, *Inorg. Chem.*, 2015, **54**, 6829.
- 3 H. Z. Li and M. S. Wong, *Org. Lett.*, 2006, **8**, 1499.
- 4 L. Guo, K. F. Li, M. S. Wong and K. W. Cheah, *Chem. Commun.*, 2013, **49**, 3597.
- 5 I. B. Berlman, In *Handbook of Fluorescence Spectra of Aromatic Molecules*; Academic Press: New York-London, 1971.